DAMAGE DEVELOPMENT ON CFRP STIFFENED PANELS IN POST-BUCKLING REGIME

Bouslama, N[1*], Maslouhi, A[1], and Jazouli, S[2]
[1]Department of Mechanical Engineering, Université de Sherbrooke (Québec), Canada
[2]Aerostructure and Engineering, Bombardier Aerospace, Montreal (Québec), Canada
* Corresponding author (Nidhal.Bouslama@Usherbrooke.ca)

Keywords*: CFRP stiffened panel, Progressive failure; Buckling and Postbuckling*

ABSTRACT

Damage tolerance in composite structure has received increasing attention, especially for aircraft primary structures. Indeed, new design approach must go beyond conservative concept and offer best structural efficiency without compromising safety requirement. Nevertheless, to deal with these challenges, a deep understanding on the damage mechanisms and reliable tools for their identification from early stage are required. In aircraft structure, stiffened composite panels are among the most-used configurations. Stiffened panels are widely introduced in the fuselage and wings thanks to their ability to withstand high load and deformation level. However, complex damage modes and nonlinear behavior in the post-buckling regime still challenging and requires better understanding.

In the current study, the buckling and post-buckling response on a hat stiffened panel made from CFRP composite material is investigated numerically to identify damage phases involved in the post-buckling process from damage initiation to final collapse. The proposed numerical model is based on progressive failure analysis (PFA) where material properties are degraded according to a specified damage law. In this study, failure criteria related to fiber, matrix and interlaminar delamination were assessed by implementing a constitutive material model using USERMAT subroutine. The analysis of these results has allowed the identification of the critical zone for damage onset and spread, which were subsequently correlated with the different buckling steps. Furthermore, experimental procedures were proposed to evaluate compression behavior of stiffened composite panels. Buckling panels will be monitored by using the digital image correlation technique (DIC) to extract the displacement and the strain field and to validate finite element modeling results.

1 INTRODUCTION

High-performance composite materials have found increasing application in aerospace industry due to their potential in terms of stiffness, strength and weight reduction. However, the recourse to composite materials raises new issues related to their design and behavior during in service life. Indeed, unlike their metallic counterparts, composite materials display a wide variety of failure mechanisms, which still much less known and require a deeper investigation.

In last few years, composite stiffened panels have received increasing interest as they are widely used in the design of principal structure elements (PSE) like fuselage, rudder and stabilizer. This structure takes profits from composite material advantages and the outstanding properties of thin-walled structure [1]. Composite panels under in-plane compression or shear loading are sensitive to bukcling failure [2]. It is acknowledged that stiffened panels can have considerable post-buckling reserve strength, these structures can still carry the load even after the appearance of the first buckling signs. Taking advantage from this phase means to be able to predict complex non-linear response and take into account the interaction between the different failures modes involved throughout this process.

The buckling and postbuckling regime of the stiffened composite panel was widely investigated under different aspects. Von Karman [3] has proposed an analytical model where a practical approach was proposed to compute the buckling load and buckling patterns. Several experimental trials carried under compression [3] [4] and shear loading [5] emphasized that the skin-stiffener separation was the main failure mode during post-buckling phase while the final failure is induced by the stringer collapse [6]. Other authors focused on the effect of defects on panel behavior and strength. Greenhalgh et al [7] focused on degradation and the decrease of the residual strength due to impact damage and embedded defect.

The increasing interest in the study of damage tolerant structures stimulated the development of numerical tools. Nowadays, finite element method (FEM) presents a powerful tool capable to handle large scale structural and predict their failure. The literature presents several damage modeling approaches based on fracture mechanics, among them, the Virtual Crack Closure Techniques (VCCT) and the Cohesive Zone Model (CZM). Both of these techniques compute the energy release rate to predict interlaminar separation. Nerveless, these techniques are intended for delamination flaws and suppose that the damage position and path are known in advance. To overcome this limitation and take into account the contribution of different other modes, progressive failure analysis (PFA) emerges as an interesting alternative to track damage sequences and progression. Based on failure criteria, this approach uses distribution of the stresses in the lamina to predict failure modes in laminate structure. Thus, if one of the criteria is fulfilled, the mechanicals properties are degraded according to a particular damage law. The progression of damage in composite laminates structures has been a focus of extensive research. Sepe et al. [8] used Hashin's criteria to predict the buckling response of two stringers panel subjected to impact damage. Ambur et al [9] studied the failure process of a stiffened panel with and without a notch under in-plane shear loading. Even if delamination criterion was neglected, numerical FE results shown a good agreement with experimental ones to mimic damage sequences. Bisagni [10] assessed the damage tolerance and collapse of a hat-stiffened composite panel by applying Larc03 failure criteria to predict fiber failure and matrix crack, while delamination damage was simulated by cohesive material model.

The aim of this study is to analyze the mechanical behavior of two hat stringers CFRP panel subjected to compression loading. The paper, details the modeling approach based on progressive failure analysis (PFA) where material properties are degraded according to a specified damage law and proposes an experimental approach based on compression testing. In order to characterize the panel behavior and to develop accurate knowledge of the possible failure modes and their interaction, damage onset and delamination propagation will be monitored both using a digital image correlation and by AE wave detection. The experimental test consists to apply uniform compression loading to the stiffened composite panel until the final collapse. The buckling and post-buckling deformation will be measured using a digital image correlation system (DIC) while the damage monitoring by using acoustic emission techniques will permit to detect damage initiation and to characterize damage accumulation under compression loading. Thereafter, experimental results will be compared to finite element model developed based on progressive failure analysis. The proposed model takes into account the major failure modes such as matrix cracking, fiber breakage, fiber-matrix shearing and interlaminar delamination. Obtained results have allowed to highlight the critical damage area and identify the sequences of damage evolution during buckling and post-buckling phases.

2 Experimental approach

2.1 CFRP stiffened panel design

The composite panel is stiffened by two hat-stringers assembled to the skin by co-cure method. The panel has 660 mm length by 382mm width and made with unidirectional CFRP material from Cytec HTS 977-2. The mechanical properties of the unidirectional lamina are detailed in Table 1. In this specimen, the skin is constituted of 12 plies with symmetric stacking sequence of $[90/45/\text{-}45/0/\text{-}45/45]_S$. The stringers are made up by 10 plies quasi-isotropic laminate with a stacking sequence of $[90/45/0/\text{-}45/0]_S$. The panel dimensions are illustrated in the Figure 1.

For compression loading, the panel is clamped at the two ends by two steel resin blocks as shown in figure 1. (b). Resin blocks are 40 mm high and 382 mm wide, which reduces the effective length of specimens to 580 mm. The resin blocks ensure embedding condition and guarantee uniform distribution of the load during the compression tests.

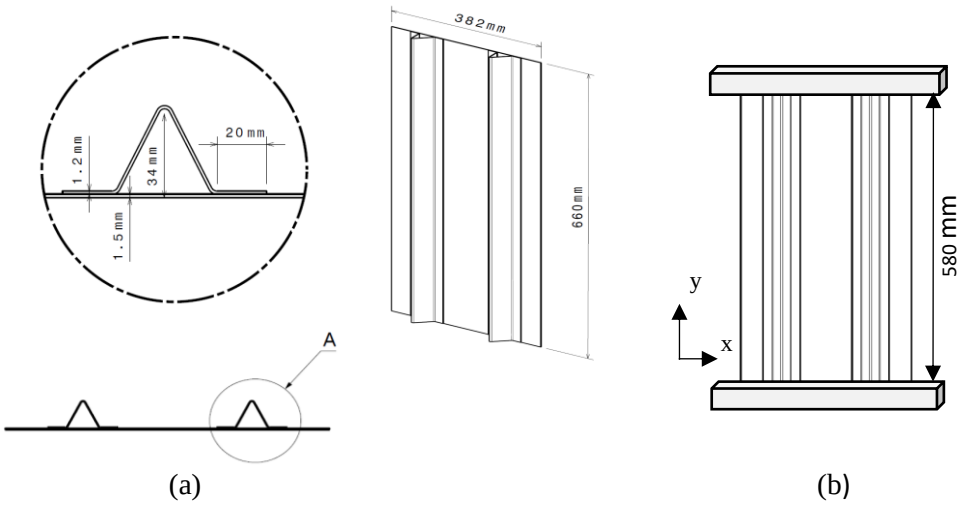

Figure 1. Geometry and dimensions of the two hat stringers panel (a) panel fixation (b).

2.2 Experimental procedures

The experimental methods mainly use the 3D digital image system VIC-3D from Correlated Solutions, to measure the strain and displacement field evolution on the surface of the specimen. This optical measurement technique allows analysis of digital images taken at different loading steps and compares them to a reference configuration. The DIC requires the application of random pattern on the surface of interest so the system can track the changes in gray value between images during loading process. For this raison, a speckle pattern was applied on the both sides of the panel as shown in Figure 2 (a). The characterization of the full field requires the use of four cameras placed on the both sides of the panel. In addition, strain gages were bonded at different positions to extract the longitudinal strain and detect the initial buckling of the panel. The gages are placed, in the skin, the flange and the stringer web. The details of strain gauge positions are given in Figure 2 (b). The damage monitoring was performed by using acoustic emission system (Mistras-µDiSP) equipped with four piezoelectric sensors (PAC) attached on the back corners of the panel with hot melt adhesive, as shown in Figure 2. (b).

(a) (b)

Figure 2. (a) Speckle pattern application on the both sides of the panel, (b) strain gages and EA sensors position.

The panel will be tested to failure using a servo-hydraulic test frame in quasi-static displacement control with a crosshead displacement fixed at 1mm/min. The experimental setup and the different monitoring tools are illustrated in Figure 3.

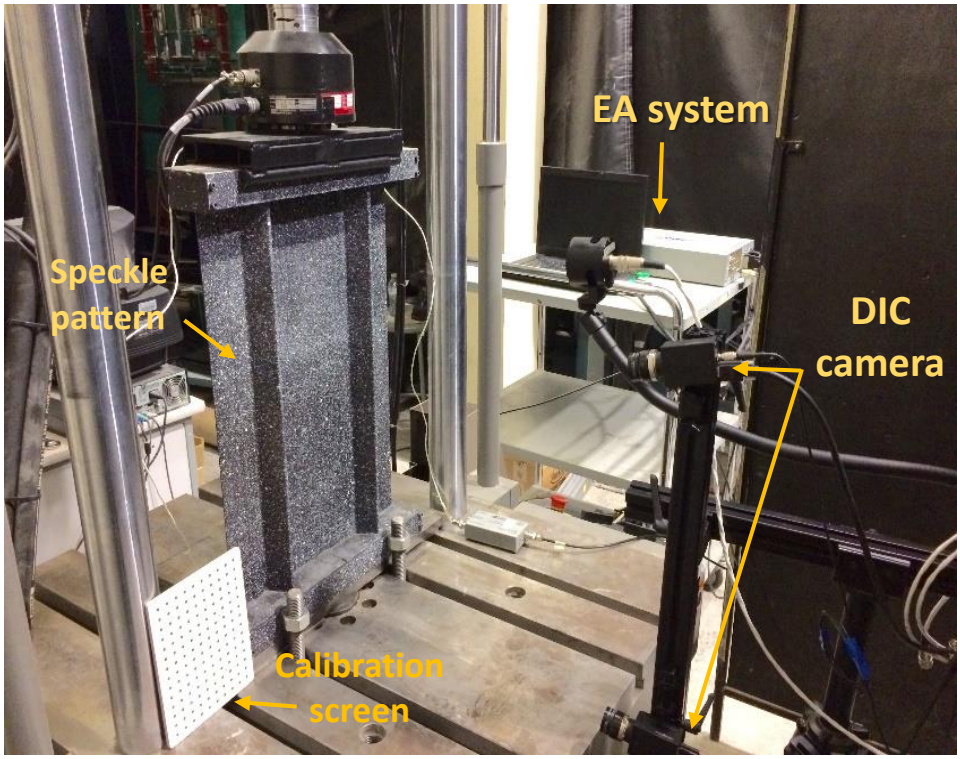

Figure 3. Experimental setup for compression testing and health monitoring tools.

3 Methodology and finite element model

3.1 Progressive damage methodology and failure criteria definition

In this paper, the progressive damage model has been implemented in ANSYS software using USERMAT subroutine. The recourse to this approach is far more effective in terms of computing time and result extraction compared to traditional post-processing routine [11]. The compilation of the FORTRAN program generates an executable file which is called by ANSYS during solution iteration. This custom subroutine requires, firstly, to establish the constitutive material law between stress and strain field by defining the Jacobin matrix $\partial\sigma/\partial\varepsilon$. Subsequently, for every loading step, the program uses strain increment to compute the new stress distribution. The stress components are used to check the predefined failure criteria list. If one of the criteria is fulfilled, the mechanical properties are instantaneous degraded according to table 2. The value of degradation coefficients depends on the damage mode, and the updated properties are stored using state variables at the end of time or load increment for each material integration point.

For this study, failure criteria proposed by Olmedo [12] and based on Chang-Chang [13] and Shokrieh-Lessard [14] development are used. These criteria combine both the contribution of out of plane stress and the nonlinear shear stress-strain relationship which is expressed by equation (1).

$$\gamma_{12} = \frac{1}{G_{12}}\,\tau_{12} + \alpha\tau_{12}^{3} \tag{1}$$

where γ and τ are respectively the strain and stress field and α is an experimental parameter [15].
The adopted failure criteria are expressed by (eq.2-5) as follow:

3.1.1 Fiber failure:

Fiber failure criteria take into account the interaction between longitudinal stress, in-plane and out of plane shear stress. The failure occurs when the following criterion is satisfied:

$$\left(\frac{\sigma_{11}}{X_T}\right)^2 + \frac{\frac{\tau_{12}^2}{G_{12}^2} + \frac{3}{4}\,\alpha\tau_{12}^4}{\frac{S_{12}^2}{2G_{12}^2} + \frac{3}{4}\,\alpha S_{12}^4} + \frac{\frac{\tau_{13}^2}{G_{13}^2} + \frac{3}{4}\,\alpha\tau_{13}^4}{\frac{S_{13}^2}{2G_{13}^2} + \frac{3}{4}\,\alpha S_{13}^4} = e_f^2 \qquad \sigma_{11} > 0 \tag{2}$$

Where X_T is replaced by X_c if $\sigma_{11} < 0$. Here S_{13} and S_{23} are the out-of-plane shear strength.

3.1.2 Matrix failure:

In addition to transverse and in plane shear stress, the following failure criterion also considers the contribution of out-of-plane shear stress.

$$\left(\frac{\sigma_{22}}{Y_T}\right)^2 + \frac{\frac{\tau_{12}^2}{2G_{12}^2} + \frac{3}{4}\,\alpha\tau_{12}^4}{\frac{S_{12}^2}{2G_{12}^2} + \frac{3}{4}\,\alpha S_{12}^4} + \frac{\frac{\tau_{23}^2}{G_{23}^2} + \frac{3}{4}\,\alpha\tau_{23}^4}{\frac{S_{23}^2}{2G_{23}^2} + \frac{3}{4}\,\alpha S_{23}^4} = e_m^2 \qquad \sigma_{22} > 0 \tag{3}$$

Where Y_T is replaced by Y_c if $\sigma_{22} < 0$.

3.1.3 Fiber–matrix shearing failure

The fiber–matrix shearing failure criterion is met if:

$$\left(\frac{\sigma_{11}}{X_C}\right)^2 + \frac{\frac{\tau_{12}^2}{G_{12}^2} + \frac{3}{4}\,\alpha\tau_{12}^4}{\frac{S_{12}^2}{2G_{12}^2} + \frac{3}{4}\,\alpha S_{12}^4} + \frac{\frac{\tau_{13}^2}{G_{13}^2} + \frac{3}{4}\,\alpha\tau_{13}^4}{\frac{S_{13}^2}{2G_{13}^2} + \frac{3}{4}\,\alpha S_{13}^4} = e_{fm}^2 \qquad \sigma_{11} < 0 \qquad (4)$$

3.1.4 Delamination

Delamination criterion used in this study is provided by the expansion of the Hashin criterion and considering the non-linear shear stress/strain behavior. The equation is given by

$$\left(\frac{\sigma_{33}}{Z_T}\right)^2 + \frac{\frac{\tau_{13}^2}{2G_{13}^2} + \frac{3}{4}\,\alpha\tau_{13}^4}{\frac{S_{13}^2}{2G_{13}^2} + \frac{3}{4}\,\alpha S_{13}^4} + \frac{\frac{\tau_{23}^2}{G_{23}^2} + \frac{3}{4}\,\alpha\tau_{23}^4}{\frac{S_{23}^2}{2G_{23}^2} + \frac{3}{4}\,\alpha S_{23}^4} = e_d^2 \qquad \sigma_{33} > 0 \qquad (5)$$

Where Z_T is replaced by Z_c if $\sigma_{33} < 0$.

As failure occurs in a ply of the laminate, the mechanical properties of each material integration point are updated using appropriate degradation parameters as defined in table (1).

Mechanical properties	$\mathbf{E_{11}}$ (GPa)	$\mathbf{E_{22}=E_{33}}$ (MPa)	$\mathbf{G_{12}}$ (MPa)	$\mathbf{G_{23} = G_{13}}$ (MPa)	$\boldsymbol{\upsilon_{12}}$	$\boldsymbol{\upsilon_{23}}$	$\boldsymbol{\upsilon_{13}}$	
	148	9500	4500	3170	0.3	0.4	0.4	
Strength (MPa)	$\mathbf{X_T}$	$\mathbf{X_C}$	$\mathbf{Y_T}$	$\mathbf{Y_C}$	$\mathbf{Z_T}$	$\mathbf{Z_C}$	$\mathbf{S_{12}}$	$\mathbf{S_{23} = S_{13}}$
	2000	1500	50	150	100	253	150	41.5

Table 1. Material properties for two delta stringers panel

Failure mode	$\mathbf{E_x}$	$\mathbf{E_y}$	$\mathbf{E_z}$	$\mathbf{G_{xy}}$	$\mathbf{G_{yz}}$	$\mathbf{G_{xz}}$	$\boldsymbol{\upsilon_{xy}}$	$\boldsymbol{\upsilon_{yz}}$	$\boldsymbol{\upsilon_{xz}}$
Fiber failure	0.14	0.4	0.4	0.25	0.35	0.2	0	0	0
Matrix failure		0.4	0.4	-	-	-	0	0	0
Fibre–matrix shearing	-	-	-	0.25	0.25	-	0	-	0
Delamination		0.4	0.4	-	0.2	-	0	0	0

Table 2. Degradation rules for the different failure modes [12]

3.2 Finite element modeling

The finite element model of the stiffened panel is performed using 3D layered SOLID 286 element with 20 nodes. These elements provide better assessment of interlaminar stress and offer the possibility to store and show results related to each layer. The material stiffness parameters and strength are introduced according table 1. The model was solved with a non-linear analysis based on Newton–Raphson algorithm.

4 Analysis of buckling behavior and damage scenario

The different phases of the panel response under compression loading are illustrated in Figure 4. Firstly, the panel under loading exhibits a linear response until 40kN with one single-wave out-of-plane deformation mode along the free edges of the skin. This phase is illustrated by pattern configuration A as shown by the figure 4. When load reaches 40 KN, a slight deviation from the linear curve is then observed, this corresponds to the apparition of the first buckling mode. This buckling mode affects only the skin and still localized within the area between two stringers. Three, then four half-waves, patterns of configuration B and C, are observed successively in the middle of the panel. By increasing compression loading, the deflection spreads and affects the both panel sides at around 62kN as shown in the figure by patterns of configuration D. At 130kN, the first buckling signs affecting the stringers are observed at point E, despite this deformation stringer remain stable and still carrying loads. The final step is characterized by stringers collapse at 162kN, where highly distorted elements are observed in both stringer webs (F).

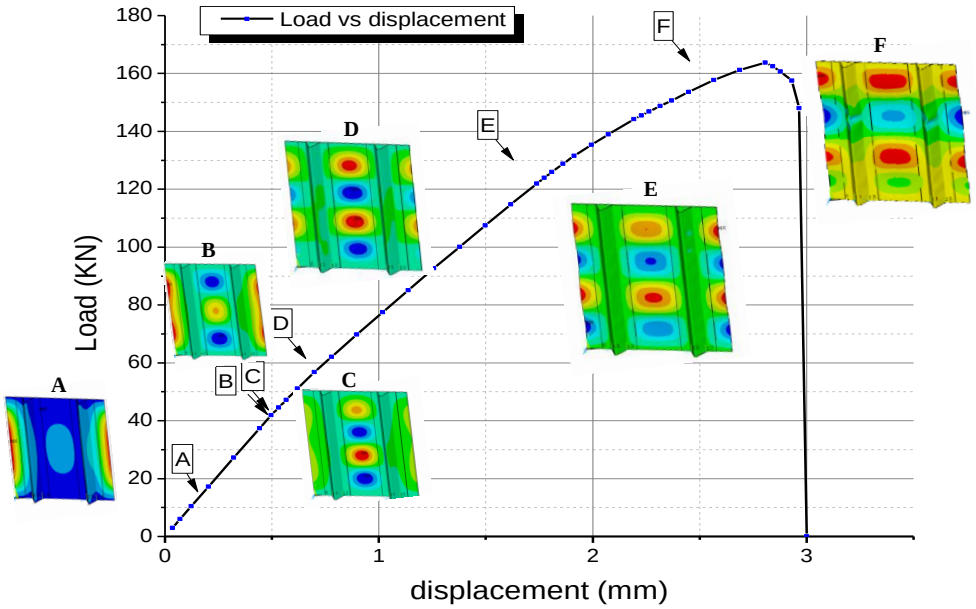

Figure 4. Mechanical behavior and out of plane response of stiffened panel with two stringers under buckling

The numerical values of strains along the loading direction ε_y are computed for different positions in the skin, flange and stringer web as it's showed previously in Figure 2. The load-strain curves computed back-to-back the skin are illustrated in Figure 5. (a). The curves show that the skin buckling occurs at around 42kN, which is characterized by a switch in the curve slope. The bifurcation between the two curves is explained by the fact that one face goes under extension, while the other one was under compression. The strain curves on the stringer flange and web are also presented in Figure 5. (b) and Figure 5. (c). By observing the web strain curve, it is possible to identify the exact value for the stringer buckling load, around 122kN, which is confirmed by the deflection observed previously by out of plane displacement as shown by configuration E.

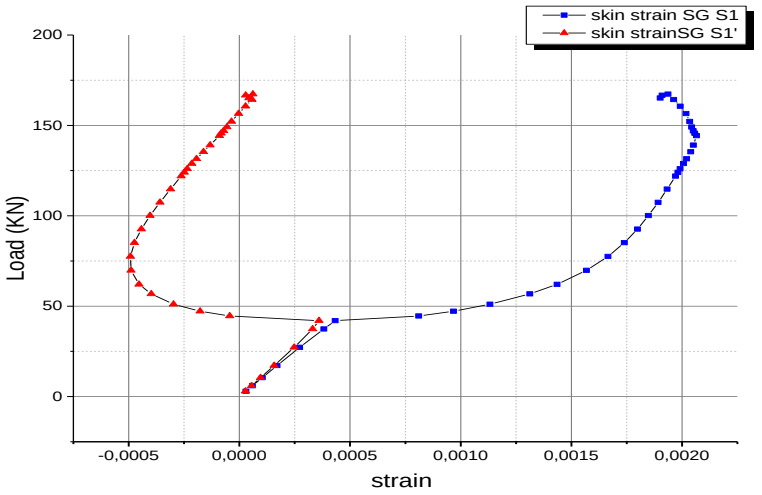

(a) Load-strain curve measured in the skin SG-S1/1'

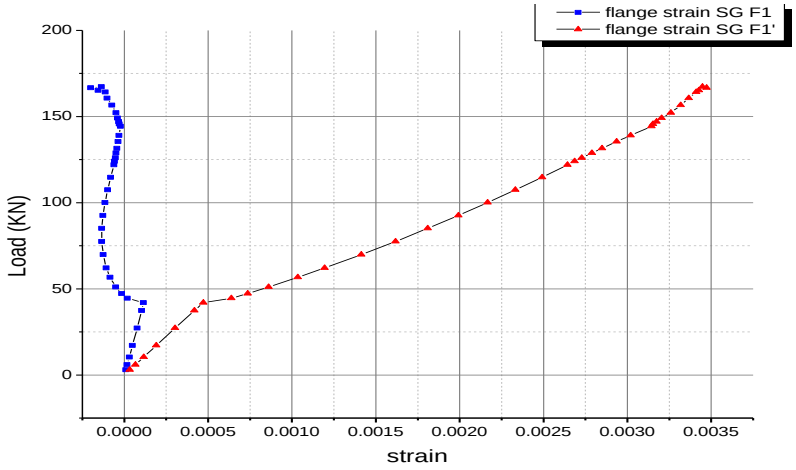

(b) Load-strain curve measured in the flange SG-F1/1'

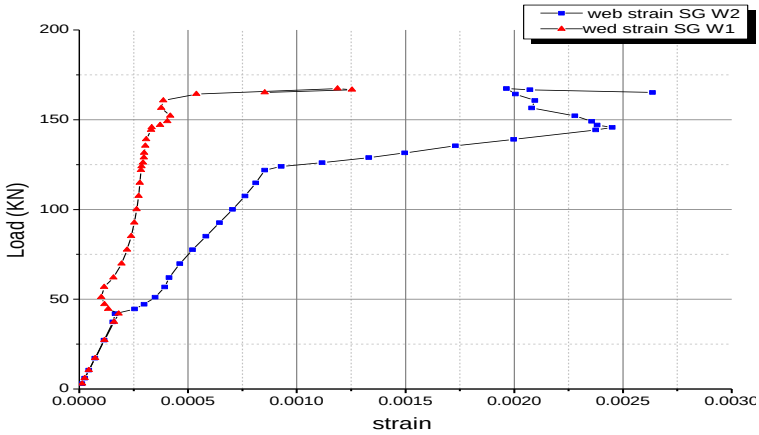

(c) Load-strain curve measured in the web SG-W1/2

Figure 5.Compression load versus strain obtained in different location in the stiffened panel by FEM analysis

The progressive failure methodology described in the paper was successfully implemented under ANSYS. The damage accumulation results are shown in Figure 6. The damage failure is expected to occur in the region with the highest negative displacement located in the middle of the panel. By observing the damage index for the three main failure modes, the progressive damage sequence was drawn in figure 6. Firstly, matrix cracks were observed just after the point D at around 62kN compressive load. Thereafter, by increasing the load, matrix damage spreads and alters larger area before the apparition of first fiber failures. Until the final failure, almost all the fiber failures still confined in the stiffener zone which provokes the final collapse of the panel. Delamination zone are typically localized in the skin-stiffener boards and in the stiffener corners. Figure 6 reports the three main failure modes observed in this panel just before the final collapse.

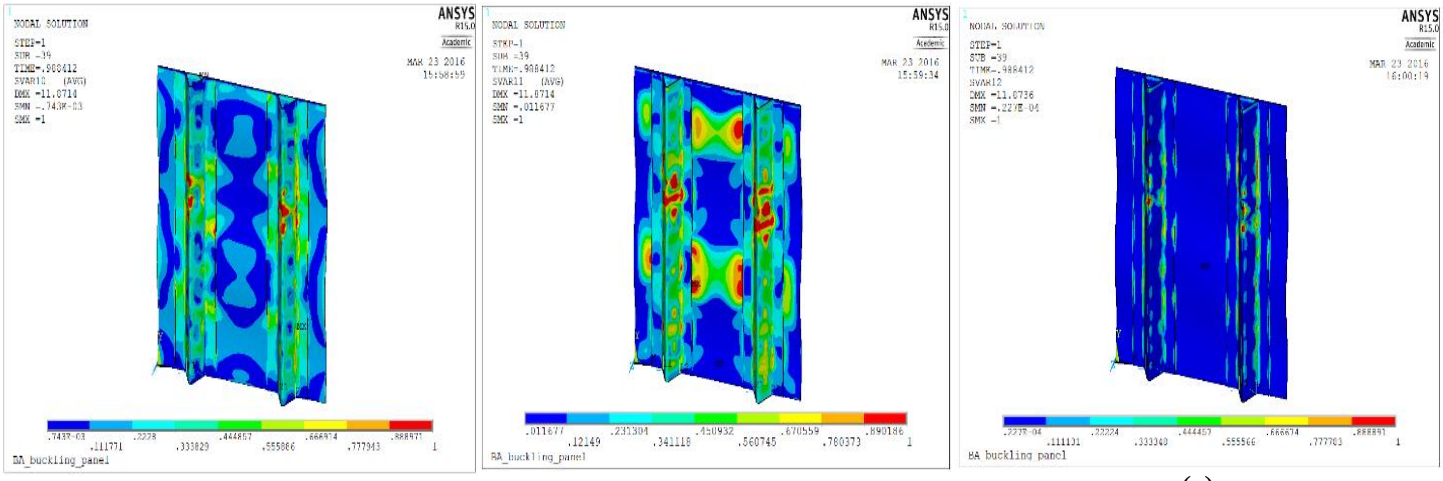

(a) (b) (c)

Figure 6. Post-buckling progressive failure map: (a) fiber breakage, (b) matrix cracking and (c) delamination

5 Conclusion

In this study, a two stringers panel made by CFRP was investigated under compression loading until final collapse. A finite element model was developed using USERMAT subroutine. The model is based on progressive failure analysis (PFA) and considers the major failure modes: fiber failure, matrix cracking, fiber-matrix shearing and delamination. The FE nonlinear analysis has allowed to compute the different buckling phases the panel go through. It also offered a detailed insight on the failure mechanisms and damage sequences. The progressive failure analysis highlight the fact that matrix cracks were the first damage mode to appear in the skin and in the stringer corners, the damage spreads in larger area by increasing the applied load until final failure occurred by stringers collapse. Also, the experimental methodology was proposed to extract the displacement full field and in-plane strain field. The DIC and AE techniques were suggested for the panel monitoring during the post-buckling stage. The experimental results and FEM validation will be presented in next paper.

Acknowledgements
The author would like to acknowledge the Consortium of Research and Innovation in Aerospace in Quebec (CRIAQ), Natural Sciences and Engineering Research Council of Canada (NSERC) and Bombardier Aerospace for their funding.

6 References

[1] R. Zimmermann, H. Klein, and A. Kling, "Buckling and postbuckling of stringer stiffened fibre composite curved panels - Tests and computations," *Compos. Struct.*, vol. 73, no. 2, pp. 150–161, 2006.

[2] E. Greenhalgh and M. Huertas Garcia, "Fracture mechanisms and failure processes at stiffener run-outs in polymer matrix composite stiffened elements," *Compos. Part A Appl. Sci. Manuf.*, vol. 35, no. 12, pp. 1447–1458, 2004.

[3] Y. Mo, D. Ge, and J. Zhou, "Experiment and analysis of hat-stringer-stiffened composite curved panels under axial compression," *Compos. Struct.*, vol. 123, pp. 150–160, 2015.

[4] S. ichi Takeda, Y. Aoki, and Y. Nagao, "Damage monitoring of CFRP stiffened panels under compressive load using FBG sensors," *Compos. Struct.*, vol. 94, no. 3, pp. 813–819, 2012.

[5] D. Ge, Y. Mo, B. He, Y. Wu, and X. Du, "Experimental and numerical investigation of stiffened composite curved panel under shear and in-plane bending," *Compos. Struct.*, vol. 137, pp. 185–195, 2016.

[6] C. Meeks, E. Greenhalgh, and B. G. Falzon, "Stiffener debonding mechanisms in post-buckled CFRP aerospace panels," *Compos. Part A Appl. Sci. Manuf.*, vol. 36, no. 7, pp. 934–946, 2005.

[7] E. Greenhalgh, C. Meeks, A. Clarke, and J. Thatcher, "The effect of defects on the performance of post-buckled CFRP stringer-stiffened panels," *Compos. Part A Appl. Sci. Manuf.*, vol. 34, no. 7, pp. 623–633, 2003.

[8] R. Sepe, A. De Luca, G. Lamanna, and F. Caputo, "Numerical and experimental investigation of residual strength of a LVI damaged CFRP omega stiffened panel with a cut-out," *Compos. Part B Eng.*, vol. 102, pp. 38–56, 2016.

[9] D. R. Ambur, N. Jaunky, and M. W. Hilburger, "Progressive failure studies of stiffened panels subjected to shear loading," *Compos. Struct.*, vol. 65, no. 2, pp. 129–142, 2004.

[10] C. Bisagni and R. Vescovini, "Assessment of the Damage Tolerance of Postbuckled Hat-Stiffened Panels using Single-Stringer Specimens," *Am. Inst. Aeronaut. Astronaut.*, vol. 48, no. 2, pp. 495–502, 2010.

[11] E. Pietropaoli, "Progressive failure analysis of composite structures using a constitutive material model (USERMAT) developed and implemented in ANSYS ??," *Appl. Compos. Mater.*, vol. 19, no. 3–4, pp. 657–668, 2012.

[12] Á. Olmedo and C. Santiuste, "On the prediction of bolted single-lap composite joints," *Compos. Struct.*, vol. 94, no. 6, pp. 2110–2117, 2012.

[13] F. Chang and K.-Y. Chang, "Laminated Composites Containing Stress Concentrations," *J. Compos. Mater.*, vol. 21, no. September, pp. 834–855, 1987.

[14] L. B. L. Mahmood M. Shokrieh, "Progressive Fatigue Damage Modeling of Composite Materials, Part I: Modeling," *J. Compos. Mater.*, vol. 34, no. 13, pp. 183–205, 2000.

[15] "Abaqus Analysis User's Manual, Simulia;," 2011.